



PARIS

Unclassified

Organisation de Coopération et de Développement Economiques  
Organisation for Economic Co-operation and Development

NEA/CSNI/R(2000)10

OLIS : 09-Mar-2000  
Dist. : 10-Mar-2000

English text only

NUCLEAR ENERGY AGENCY  
COMMITTEE ON THE SAFETY OF NUCLEAR INSTALLATIONS

## CARBON MONOXIDE - HYDROGEN COMBUSTION CHARACTERISTICS IN SEVERE ACCIDENT CONTAINMENT CONDITIONS

Final report

*Prepared by R.K. Kumar and G.W. Koroll, AECL, Canada; M. Heitsch, GRS, Germany and E. Studer, IPSN, France. In consultation with CSNI-PWG4 Task Group on Severe Accident Phenomena in the Containment*

88481

Document complet disponible sur OLIS dans son format d'origine  
Complete document available on OLIS in its original format

NEA/CSNI/R(2000)10  
Unclassified

English text only

## **ORGANISATION FOR ECONOMIC CO-OPERATION AND DEVELOPMENT**

Pursuant to Article 1 of the Convention signed in Paris on 14th December 1960, and which came into force on 30th September 1961, the Organisation for Economic Co-operation and Development (OECD) shall promote policies designed:

- to achieve the highest sustainable economic growth and employment and a rising standard of living in Member countries, while maintaining financial stability, and thus to contribute to the development of the world economy;
- to contribute to sound economic expansion in Member as well as non-member countries in the process of economic development; and
- to contribute to the expansion of world trade on a multilateral, non-discriminatory basis in accordance with international obligations.

The original Member countries of the OECD are Austria, Belgium, Canada, Denmark, France, Germany, Greece, Iceland, Ireland, Italy, Luxembourg, the Netherlands, Norway, Portugal, Spain, Sweden, Switzerland, Turkey, the United Kingdom and the United States. The following countries became Members subsequently through accession at the dates indicated hereafter: Japan (28th April 1964), Finland (28th January 1969), Australia (7th June 1971), New Zealand (29th May 1973), Mexico (18th May 1994), the Czech Republic (21st December 1995), Hungary (7th May 1996), Poland (22nd November 1996) and the Republic of Korea (12th December 1996). The Commission of the European Communities takes part in the work of the OECD (Article 13 of the OECD Convention).

## **NUCLEAR ENERGY AGENCY**

The OECD Nuclear Energy Agency (NEA) was established on 1st February 1958 under the name of the OEEC European Nuclear Energy Agency. It received its present designation on 20th April 1972, when Japan became its first non-European full Member. NEA membership today consists of 27 OECD Member countries: Australia, Austria, Belgium, Canada, Czech Republic, Denmark, Finland, France, Germany, Greece, Hungary, Iceland, Ireland, Italy, Japan, Luxembourg, Mexico, the Netherlands, Norway, Portugal, Republic of Korea, Spain, Sweden, Switzerland, Turkey, the United Kingdom and the United States. The Commission of the European Communities also takes part in the work of the Agency.

The mission of the NEA is:

- to assist its Member countries in maintaining and further developing, through international co-operation, the scientific, technological and legal bases required for a safe, environmentally friendly and economical use of nuclear energy for peaceful purposes, as well as
- to provide authoritative assessments and to forge common understandings on key issues, as input to government decisions on nuclear energy policy and to broader OECD policy analyses in areas such as energy and sustainable development.

Specific areas of competence of the NEA include safety and regulation of nuclear activities, radioactive waste management, radiological protection, nuclear science, economic and technical analyses of the nuclear fuel cycle, nuclear law and liability, and public information. The NEA Data Bank provides nuclear data and computer program services for participating countries.

In these and related tasks, the NEA works in close collaboration with the International Atomic Energy Agency in Vienna, with which it has a Co-operation Agreement, as well as with other international organisations in the nuclear field.

## **CSNI**

The NEA Committee on the Safety of Nuclear Installations (CSNI) is an international committee made up of senior scientists and engineers, with broad responsibilities for safety technology and research programmes, and representatives from regulatory authorities. It was set up in 1973 to develop and co-ordinate the activities of the NEA concerning the technical aspects of the design, construction and operation of nuclear installations insofar as they affect the safety of such installations. The Committee's purpose is to foster international co-operation in nuclear safety amongst the OECD Member countries. CSNI's main tasks are to exchange technical information and to promote collaboration between research, development, engineering and regulation organisations; to review the state of knowledge on selected topics of nuclear safety technology and safety assessments, including operating experience; to initiate and conduct programmes to overcome discrepancies, develop improvements and reach consensus on technical issues; to promote co-ordination of work, including the establishment of joint undertakings.

## **PWG4**

CSNI's Principal Working Group on the Confinement of Accidental Radioactive Releases (PWG4) has been given two tasks: containment protection, and fission product retention. Its role is to exchange information on national and international activities in the areas of severe accident phenomena in the containment, fission product phenomena in the primary circuit and the containment, and containment aspects of severe accident management. PWG4 discusses technical issues/reports and their implications, and the results of International Standard Problem (ISP) exercises and specialist meetings, and submits conclusions to the CSNI. It prepares Technical Opinion Papers on major issues. It reviews the main orientations, future trends, emerging issues, co-ordination and interface with other groups in the field of confinement of accidental radioactive releases, identifies necessary activities, and proposes a programme of work to the CSNI.

## **SAC**

The Task Group on Severe Accident Phenomena in the Containment (SAC) is a specialised extension of PWG4. Its main tasks are to exchange information, discuss results and programmes, write state-of-the-art reports, organise specialist workshops, and perform ISP exercises in the field of severe accident phenomenology.



## TABLE OF CONTENTS

<b>INTRODUCTION</b> .....	7
<b>RESULTS</b> .....	9
Flammability limits .....	9
Ignition temperatures .....	10
Autoignition .....	10
Hot-surface ignition.....	11
Burning velocities .....	11
Combustion in vessels.....	11
Combustion pressures in closed vessels .....	12
Combustion pressures in vented vessels.....	12
Detonation cell widths.....	12
Induction time calculations .....	13
Determination of the cell width proportionality constant—A.....	14
Effect of initial temperature on cell width.....	14
Effect of carbon monoxide addition to dry hydrogen-air mixtures .....	15
Effect of steam addition on cell width.....	15
Effect of carbon monoxide addition on cell width for hydrogen-air-steam mixtures .....	15
Inference from calculated cell widths with CO addition.....	16
<b>DISCUSSION</b> .....	17
Gaps in knowledge .....	17
Safety implications of CO in containment .....	17
Flammability limits .....	17
Ignition temperatures.....	17
Burning velocities and combustion in vessels.....	18
Detonability .....	18
<b>SUMMARY</b> .....	19
<b>REFERENCES</b> .....	21
<b>TABLE AND FIGURES</b> .....	23
<b>APPENDIX A. Consideration of carbon monoxide in French severe accident studies</b> .....	37



## INTRODUCTION

Carbon monoxide can be produced in severe accidents from interaction of ex-vessel molten core with concrete. Depending on the particular core-melt scenario, the type of concrete and geometric factors affecting the interaction, the quantities of carbon monoxide produced can vary widely, up to several volume percent in the containment. Carbon monoxide is a combustible gas. The carbon monoxide thus produced is in addition to the hydrogen produced by metal-water reactions and by radiolysis, and represents a possibly significant contribution to the combustible gas inventory in the containment. Assessment of possible accident loads to containment thus requires knowledge of the combustion properties of both CO and H<sub>2</sub> in the containment atmosphere. Extensive studies have been carried out and are still continuing in the nuclear industry to assess the threat of hydrogen in a severe reactor accident. However the contribution of carbon monoxide to the combustion threat has received less attention. Assessment of scenarios involving ex-vessel interactions require additional attention to the potential contribution of carbon monoxide to combustion loads in containment, as well as the effectiveness of mitigation measures designed for hydrogen to effectively deal with particular aspects of carbon monoxide.

The topic of core-concrete interactions has been extensively studied; for more complete background on the issue and on the physical/thermalhydraulics phenomena involved, the reader is referred to Proceedings of CSNI Specialists Meetings (Ritzman, 1987; Alsmeyer, 1992) and a State-of-Art Report (European Commission, 1995). The exact amount of carbon monoxide present in a reactor pit or in various compartments (or rooms) in a containment building is specific to the type of concrete and the accident scenario considered. Generally, concrete containing limestone and sand have a high percentage of CaCO<sub>3</sub>. Appendix A provides an example of results of estimates of CO and CO<sub>2</sub> production from a study for French reactors. For limestone-sand concrete, CO could be present in significant quantities (6% to 8%). For siliceous concrete, on the other hand, the CO concentration is generally small, of the order of 1%. Combustible gas generation (carbon monoxide and ex-vessel hydrogen) from core-concrete interactions is predicted in available codes (i.e., CORCON, WECHSL) but results are also highly plant specific. For this reason, the generation of CO is not examined in detail in this report, beyond defining a relevant range of compositions that bound the possible cases.

This report reviews the knowledge base on CO/H<sub>2</sub> combustion from the perspective of assessing the potential combustion threat in containment during a severe reactor accident. Most aspects of classical combustion behaviour are discussed, including flammability limits, burning velocities, pressure development and detonability. Since CO and H<sub>2</sub> co-exist with copious quantities of CO<sub>2</sub> and steam in containment, diluent effects of CO<sub>2</sub> and steam on H<sub>2</sub>/CO combustion properties are also examined, where known. Where evident gaps in knowledge exist, they are identified and the safety implications of the resulting uncertainties are discussed.



## RESULTS

### Flammability limits

The flammability limit is the experimentally-determined minimum concentration of fuel (lean limit) or oxidant (rich limit) required for self-sustaining flame propagation at a specified initial pressure and temperature. The flammability limit is of primary interest in safety assessments as an absolute indication of the existence of a combustion hazard and the main reference point in defining a safety margins for a combustion hazard.

There is extensive experimental data on the flammability limits of CO-H<sub>2</sub> mixtures in air. From the early works of many investigators, the flammability limits of wet CO in air is known to be 12.5% CO at the lean limit and 74% CO at the rich limit (Coward & Jones, 1952). A pure CO/air mixture may not burn at NTP because of the absence of chain carriers and chain branching reactions essential for flame propagation. A small amount of water vapour or hydrogen will ensure production of chain carriers; when present in small quantities, the effects of hydrogen and water vapour have about the same effect on CO oxidation kinetics. In containment, water vapour and, possibly, hydrogen are essentially assured so the dry flammability limit of CO is not relevant.

The flammability limit of H<sub>2</sub> in air is 4% H<sub>2</sub> at the lean limit for upward propagation and 75% H<sub>2</sub> at the rich limit for both upward and downward propagation. Addition of up to 12.5% CO to a lean-limit H<sub>2</sub>-air mixture is not expected to change the flammability limits of H<sub>2</sub>-air mixtures. Thus all mixtures containing >4% H<sub>2</sub> or >12.5% CO will burn provided the oxygen limit is not reached. The oxygen limit is the same, about 5%, for both CO/air (with traces of H<sub>2</sub> or H<sub>2</sub>O) and H<sub>2</sub>/air mixtures. Karim *et al.* (1985) have obtained flammability data in air for several binary fuel mixtures including CO and H<sub>2</sub>. Figure 1 shows the flammability limits of CO-H<sub>2</sub> mixtures reproduced from Karim *et al.* (1985). Their results indicate that LeChatelier's Rule<sup>1</sup> is surprisingly accurate in predicting the limits. In fact, the discrepancy between the measured and calculated values is less than 1%.

Flammable range of most mixtures widens with increasing temperature. This has been observed for CO-H<sub>2</sub> mixtures also. Experiments performed by Hustad and Sonju (1988) over a temperature range of 200 to 420°C indicate that Le Chatelier's Rule is quite accurate over the range of investigation.

Since both lean and rich limits for upward and downward propagation are available over a wide range of initial temperatures for both H<sub>2</sub>-air and CO-air mixtures (Cohen, 1992), and since Le Chatelier's rule has been shown to be quite accurate, the flammability limits for all CO-H<sub>2</sub> mixtures in oxygen and air atmospheres can be calculated.

---

1. Le Chatelier's rule (Coward and Jones, 1952) states that the flammability limit,  $L_m$ , of a mixture of fuels can be deduced from the relationship,  $1/L_m = \sum_i (y_i / L_i)$ , for  $i = 1, \dots, n$ , where  $y_i$  is the volume fraction of the fuel  $i$ .  $L_i$  is the flammability limit of the fuel  $i$ .

The flammability limits are also influenced by the amount and type of diluent. Whereas significant data on the effects of N<sub>2</sub> and CO<sub>2</sub> exist, there is no data on the effects of steam on the flammability limits of CO-H<sub>2</sub> mixtures. However, work of Karim *et al.* (1985) indicates that Le Chatelier's rule predicts the effect of N<sub>2</sub> and CO<sub>2</sub> diluents reasonably accurately. Karim *et al.* (1985) also state that Le Chatelier's rule produces slightly less accurate results for CO<sub>2</sub> diluent than that for N<sub>2</sub> diluent. It is expected that the accuracy of prediction of limits with steam diluent would not be significantly different from that with CO<sub>2</sub>, although CO<sub>2</sub> has a greater thermal effect on the flammability limits than steam. However, as stated, data is lacking to confirm the effects of steam diluent on flammability limits of CO-H<sub>2</sub> mixtures.

Typical calculations using Le Chatelier's rule for some sample mixtures are shown in Table 1.

**Table 1: Flammability limits for H<sub>2</sub>-CO mixtures**

H <sub>2</sub> /CO ratio in the Fuel Mixture (%)	Lean Limit (%)	H <sub>2</sub> in the Mixture (%)	CO in the Mixture (%)
1:3	8.16	2.04	6.12
1:1	6.06	3.03	3.03
3:1	4.82	3.61	1.20

An alternative approach to the determination of flammability limits for H<sub>2</sub>/CO/Air/CO<sub>2</sub>/H<sub>2</sub>O has been proposed by Snoeck (1997). In this approach, the flammability limits are determined by fitting a curve through known flammability values. It is assumed that the flammability limits of H<sub>2</sub>/CO/Air/CO<sub>2</sub>/H<sub>2</sub>O mixture can be estimated from the relationship

$$y = b^{-1} [y_1^{-a} + y_r^{-a}]^{-1/a}$$

where

$$y_1 = m_1 x + b_1$$

$$y_r = m_r x + b_r$$

x is the flammability limit, y is the diluent concentration, and a, b, b<sub>1</sub>, b<sub>r</sub>, m<sub>1</sub>, and m<sub>r</sub> are constants, to be determined from experimental data.

## Ignition temperatures

### *Autoignition*

Autoignition temperature is the temperature (at a given pressure and mixture composition) at which a combustible gas mixture will spontaneously ignite. It is of interest in safety assessments in the evaluation of mechanisms for initiating combustion.

Autoignition temperatures of H<sub>2</sub> and CO are separately known and are on the order of 580°C and 800°C, respectively. There is no unique autoignition temperature for CO-O<sub>2</sub> or CO-air mixtures. Even small amounts of moisture or hydrogen can drastically alter the autoignition temperature of CO-O<sub>2</sub> or CO-air mixtures. At present, there is not much information available on the autoignition behavior of CO-H<sub>2</sub> mixtures. Addition of small quantities of CO to H<sub>2</sub>/air mixture is not expected to change the autoignition temperature of the mixture significantly. However, addition of significant amount of CO may affect the

ignition temperatures. Since the details of chemical kinetics for CO-H<sub>2</sub>-O<sub>2</sub> systems have been well established (Maas and Warnatz, 1988; Rawlins and Gardiner, 1974), the autoignition temperatures for CO-H<sub>2</sub> mixtures in O<sub>2</sub> or air can be determined analytically using the existing kinetic codes. Autoignition temperature is not of primary interest in containment safety studies.

### ***Hot-surface ignition***

Hot-surface ignition is similar to autoignition in behaviour and is of somewhat greater interest as it relates to effectiveness of potential igniting sources such as glow plug-type ignitors. Hot surface ignition temperatures are higher than autoignition temperatures by a widely varying amount, depending of the geometry of the surface. The effect of CO additions to H<sub>2</sub>-air and H<sub>2</sub>-O<sub>2</sub> mixtures on the hot-surface ignition temperature, though more complex than simple autoignition, can also be determined analytically using kinetic codes with mass-transfer included (Kumar, 1991). Hot-surface ignition temperatures are also of interest in assessing the performance of passive autocatalytic recombiners (PARS).

### **Burning velocities**

The burning velocity is the velocity of the flame relative to the velocity of the gas in which it propagates. Laminar burning velocity is a fundamental property of a combustible gas mixture. Burning velocity is strongly affected by turbulence; turbulence effects are a source of uncertainty in determining burning velocities for any gas mixture in real systems where turbulence is not well quantified. Burning velocities are a key input parameter in codes that calculate combustion pressure development and are thus important in safety assessments.

Laminar burning velocities of CO in moist air and CO in moist (O<sub>2</sub> + N<sub>2</sub>) for a range of O<sub>2</sub>/N<sub>2</sub> are known (Lewis & von Elbe, 1987). The burning velocities of H<sub>2</sub>/air/steam mixtures are also widely available (ref.) and mixing rules for diluent effects on burning velocity are available. Burning velocities of hydrogen are about an order of magnitude higher than those for carbon monoxide. However, there is very little data on the burning velocities of H<sub>2</sub>/CO and H<sub>2</sub>/CO/steam mixtures in air.

Addition of small amounts of hydrogen in CO/air mixtures has been studied and is observed to affect the laminar burning velocity significantly (though the case of high CO and low H<sub>2</sub> concentrations is of less interest in containment), as intuitively expected from the very high burning velocity of the hydrogen additive. For the more relevant opposite case, addition of small amounts of CO to a H<sub>2</sub>-air mixture, it is not clear whether the burning velocities would be significantly affected. It is reasonable to assume, based on observations of adding small amounts of hydrocarbons, that the burning velocity of H<sub>2</sub>-air mixture should not be significantly affected by the presence of small amounts of CO in lean hydrogen-air mixtures.

The burning velocities of CO/H<sub>2</sub>/H<sub>2</sub>O/air system can be calculated from the various burning velocity codes currently available (Warnatz, 1979; Stephenson and Taylor, 1973). However, these codes have a limited range of applicability and cannot be used below a certain fuel concentration. Unfortunately, the region of interest in reactor safety includes low CO and H<sub>2</sub> concentrations, which have the largest uncertainty in the burning velocity calculation. The burning velocities at low CO concentrations in relevant mixtures with hydrogen have to be determined experimentally.

### **Combustion in vessels**

The combustion pressure development is of primary interest in safety assessments and is usually calculated by combustion models in containment codes. The burn calculations are validated using data from large-scale engineered tests. Pressure development under conditions of constant volume (closed

vessels) and in volumes separated by openings (vented combustion) are relevant to containment safety assessments. The vented combustion case is most relevant to assessment of actual accident progression and the integrity of containment subvolumes.

### ***Combustion pressures in closed vessels***

Constant volume combustion pressures are bounded by the adiabatic isochoric complete combustion (AICC) pressure, which is essentially a thermodynamic calculation. The AICC pressures for CO-H<sub>2</sub>-Air mixtures (see Figure 2) can be calculated readily using the NASA CEC72 (Gordon & McBride, 1971). Thus calculated, combustion pressures are significantly affected by the presence of CO in direct proportion to the contribution made to the energy content of the gas volume. (I.e., while 5% CO will not burn in air, when added to a 10% hydrogen-air mixture would definitely burn, adding its energy to increase the pressure of the hydrogen burn. Thus, addition of 5% CO to a 10% H<sub>2</sub>-air mixture, would increase the adiabatic isochoric complete combustion (AICC) pressure from 4.3 atm. to 5.7 atm.)

### ***Combustion pressures in vented vessels***

Vented combustion involves complex interplay between the burning velocity and the particular geometry of the enclosures. Thus the calculation of vented combustion pressures requires reliable burning velocity inputs and extensive large-scale validation. No large-scale experimental data, either in vented or non-vented vessels, have been found for CO or CO/H<sub>2</sub> mixtures. As the CO fraction increases and the vented combustion behaviour departs from the pure hydrogen case, the validity of the predictions of pressure development will increasingly come into question. Even a relatively small number of large-scale tests with atmospheres containing prototypical CO/H<sub>2</sub> mixtures would significantly improve validity of predictions.

### **Detonation cell widths**

Detonation cell width is a fundamental physico-chemical property that determines many detonation characteristics of a combustible mixture and is used, indirectly, to define the composition limits of detonability. Many of the detonation characteristics – such as transmission of detonation through orifices, channels, and obstacle arrays – depend on the detonation cell width of the mixture. The detonation cell size also determines the energy required for direct initiation of detonation in a given mixture and the critical tube diameter for transition from a planar to a spherical detonation. Because of the importance of detonation cell width in safety assessment and the magnitude of potential for contributions by CO, it is examined in somewhat greater detail here.

Detonation cell widths for many fuel-oxygen and fuel-air mixtures have been reported by various investigators (Strehlow and Engel, 1968; Westbrook, 1982; Bull *et al.*, 1982). Tieszen *et al.* (1985) have experimentally determined the detonation cell widths in hydrogen-air-steam mixtures, relevant to nuclear reactor safety. Kumar (1990) has determined detonation cell widths in stoichiometric hydrogen-oxygen-steam mixtures, relevant to CANDU<sup>®</sup> reactor safety. Whereas considerable experimental detonation cell size data exist for hydrogen-air-steam mixtures, there does not appear to be experimental data for hydrogen-carbon monoxide-steam-air mixtures. This omission is probably due to lack of interest in carbon monoxide as a fuel and also because of the difficulty in performing experiments involving carbon monoxide—carbon monoxide is a highly toxic gas and requires special precautions in handling and storage.

---

<sup>®</sup> CANDU is a registered trademark of the Atomic Energy of Canada Limited.

Semi-empirical analytical models in which the detonation cell width is seen to be proportional to the induction zone length of a planar detonation wave have been successfully used to estimate the cell widths. In these models it is assumed that the transverse length of the cell (cell width),  $\lambda$ , is proportional to the induction length,  $l$ , which is a product of the induction time,  $t_s$ , and the post-shock gas velocity,  $V_s$ . That is,  $\lambda \sim t_s V_s = A t_s V_s$ , where  $A$  is a constant that depends on factors such as fuel type and the type and amount of diluent used. Whereas  $V_s$  can be determined readily from the thermodynamic equilibrium calculations, determination of the induction time requires detailed chemical kinetic models.

Magzumov *et al.* (1995) theoretically studied the effect of carbon monoxide addition on the detonation sensitivity of dry hydrogen-air mixtures, using detailed carbon monoxide kinetics. They observed that addition of CO to a hydrogen-air mixture increases the detonation sensitivity of the mixture (detonation sensitivity  $\sim 1/\lambda$ ). This paper deals with the analytical determination of detonation cell widths in hydrogen-carbon monoxide-air-steam mixtures that are relevant to LWR safety using the ZND detonation model.

### **Induction time calculations**

As mentioned earlier, the detonation cell width is related to the induction zone length which, in turn, depends on the chemical induction time. The induction time can be calculated once the conditions behind the shock are known, assuming that details of the reaction kinetics are known. In the present work, the detonation Mach number was calculated using the standard NASA code (Gordon and McBride, 1971), assuming equilibrium composition. Post-shock gas conditions, such as temperature and pressure required for determining the induction time, were then calculated using normal shock relationships. Details of the reaction mechanism used in the induction time calculations are the same as those given in Kumar (1990), with some additional reactions for CO oxidation (e.g., CO, CHO, CH<sub>2</sub>O, CO<sub>2</sub>). The additional reactions used are shown in Table 2. Rate constants for CO oxidation reactions were selected from Gardiner (1984). For some reactions, the rate constants were not available; a zero value was assumed for these constants. The third-body efficiencies for various gas molecules were the same as those used in Kumar (1989), except for CO which was assumed to be unity.

Validation of the induction time model used in the present calculations is reported in Kumar (1990). During computations, the time steps were automatically calculated to maintain the solution stable and converged. To ascertain the convergence of solutions, the induction times were calculated using initial time steps that differed by an order of magnitude. No significant differences in the calculated induction times were found.

One of the important considerations in calculating the cell width is the determination of the induction time or induction length. Shepherd (1985) used Raleigh line flow and defined the induction length as the distance corresponding to a down stream Mach number of 0.75. Kumar (1990) defined induction time as the time corresponding to a temperature rise that is equal to a specified fraction of the adiabatic temperature rise. A similar definition is adopted here. Induction time is defined as the instant corresponding to a temperature rise of 5% of the adiabatic temperature rise. Incidentally, this value was found to correspond to the instant of highest rate of temperature rise due to chemical reactions occurring behind the shock wave.

Figure 3 shows a typical plot of the gas temperature plotted as a function of time. It is seen from the figure that choosing any temperature rise in the range of 5% to 90% of the adiabatic temperature rise will give nearly the same induction time. The value of the proportionality constant  $A$  depends on the induction time definition.

### ***Determination of the cell width proportionality constant—A***

Before the cell widths in hydrogen-air-steam and hydrogen-carbon monoxide-air-steam mixtures can be estimated, the proportionality constant  $A$  should be established from experimentally measured cell widths for hydrogen-air mixtures. Figure 4 shows the measured and calculated cell widths plotted against hydrogen concentration. Although a single value of  $A$  is not adequate over the whole range, a reasonably good agreement between the measured and calculated values was obtained for  $A = 27$ . This value is in rough agreement with  $A$  values of 22 and 20, respectively, suggested by Shepherd (1985) and Westbrook and Urtiew (1982).

A reference to Figure 4 indicates that the estimated cell widths are lower than the measured values for very lean and very rich mixtures. It should be noted that in hydrogen-oxygen-diluent mixtures, the cells are not uniform (except for argon and helium diluents) and the extreme cell sizes observed in a single experiment differ by as much as 30% to 50% from the mean values (Kumar, 1990). In view of this difference, agreement between the measured and calculated values, shown in Figure 4, can be considered satisfactory.

It was pointed out previously that the factor  $A$  depends on the type of fuel. Also, Kumar (1990) pointed out that, for stoichiometric hydrogen-oxygen-diluent mixtures, the factor  $A$  depends strongly on the diluent concentration. It is therefore not clear whether the value of  $A$  derived from the measured cell widths for hydrogen-air mixtures can be satisfactorily applied to hydrogen-air-steam and hydrogen-carbon monoxide-air-steam mixtures. However, a reference to Guirao *et al.* (1989) indicates that a good agreement between measured and calculated sizes was obtained for hydrogen-air-steam mixtures over a wide range of hydrogen and steam concentrations.

The concentration of carbon monoxide present in the combustible pockets of hydrogen-carbon monoxide-air-steam mixtures during a postulated core-melt accident is not expected to be large. For the present calculations, carbon monoxide concentrations of 5% and 10% (by volume) were used. For these low concentrations of CO, it is reasonable to assume that CO addition will not significantly affect the value of  $A$ . Thus a constant value of  $A = 27$  was used in the present calculations.

### ***Effect of initial temperature on cell width***

As the initial temperature increases, the post-shock gas (unburned) temperature increases, and since the reaction rates have an exponential dependence on the gas temperature, it is expected that the induction time should decrease. However, as the initial temperature increases, the detonation Mach number decreases. This causes a reduction in the post-shock gas pressure. Thus the net effect of an increase in the initial temperature on induction time is small. Since the post-shock gas velocity is not significantly affected by the initial temperature, initial gas temperature has only a small effect on the cell width. This observation can be clearly seen from Figure 5, which compares the calculated cell widths at 298 K and 373 K for a range of hydrogen concentrations. Over the temperature range investigated, the cell width decreases slightly as the temperature increases. Experiments performed by Kumar (1990) in a 15-cm-diameter detonation tube had indicated that for stoichiometric hydrogen-oxygen-diluent mixtures, an increase in the initial temperature from 20°C to 100°C did not significantly affect the measured cell widths.

### ***Effect of carbon monoxide addition to dry hydrogen-air mixtures***

Although pure carbon monoxide is difficult to burn in air or oxygen (Lewis and von Elbe, 1987), the presence of impurities containing hydrogen can significantly enhance the rate of CO oxidation reactions. Thus one may expect CO to participate in the chemical reactions when added to hydrogen-air mixtures.

Figure 6 shows the effect of CO addition on induction times for a range of hydrogen concentration. The effect of CO on induction time depends on the hydrogen-air stoichiometry. In the 25% to 45% hydrogen concentration range, addition of CO does not appear to have much effect on the induction time. For lean mixtures, the induction time decreases with CO addition. This decrease occurs because, in lean hydrogen-air mixtures, there is excess oxygen available for CO oxidation, resulting in a significant increase in the concentration of chain carriers and energy release to the gas. These effects cause the induction time to decrease. For rich mixtures, on the other hand, the oxygen available is limited, and both hydrogen and CO compete for the available oxygen. Thus addition CO tends to increase the induction time.

The effect of CO addition on the cell width is similar in trend to that on the induction time. Addition of CO significantly lowers the cell width for lean hydrogen-air mixtures and increases the cell widths for rich hydrogen-air mixtures. Figure 7 shows, for example, that addition of 5% CO to a 15% hydrogen-air mixture reduces the cell width by a factor of ~4 and that addition of 10% CO decreases the cell width by a factor of ~8. For rich mixtures, additions of 5% and 10% CO increase the cell width by factors of 2 and 3 respectively. Thus addition of CO to a lean hydrogen-air mixture increases its detonation sensitivity; for rich hydrogen-air mixtures, the opposite is true. These results are in good agreement with those reported by Magzumov *et al.* (1995).

### ***Effect of steam addition on cell width***

The effect of steam addition is first to displace the oxygen the mixture and second to participate in the chemical reactions. Also, being a trimolecular gas, steam increases the specific heat of the mixture and reduces the post-compression gas temperature. Kumar (1989) has shown that because of its high third-body effectiveness, steam is very effective in quenching chain reactions. The net result of these effects is that both the induction time and the cell width increase as the steam concentration increases. Figure 8 shows the cell width plotted as a function of hydrogen concentration for steam concentrations of 0%, 10% and 20%. It is seen that steam significantly narrows the detonable range. Addition of steam reduces the oxygen available for combustion and moves the stoichiometry to lower hydrogen concentrations. On a dry basis, cell size minima still occurs for stoichiometric mixtures. These results are in good qualitative agreement with the experimental values reported in Guirao *et al.* (1989).

### ***Effect of carbon monoxide addition on cell width for hydrogen-air-steam mixtures***

Figure 9 shows the effect of 5% and 10% CO addition to hydrogen-air-10% steam mixtures. The cell width behaviour with CO addition to mixtures containing steam is similar to that observed in dry mixtures. However, the effect of CO addition for hydrogen-air-steam mixtures appears to be more pronounced than that for dry mixtures. The cell width minima location shifts towards lower hydrogen concentrations with an increase in the CO concentration. A similar behaviour is observed for hydrogen-air-steam mixtures containing 20% steam (see Figure 10). Figures 5, 7, and 8 indicate that variations in the cell widths are caused by the changes in the hydrogen stoichiometry.

***Inference from calculated cell widths with CO addition***

If the results are plotted on the basis of overall stoichiometry, there does not appear to be any observable change in the cell width with CO addition (see Figure 10). Since hydrogen and CO both have the same stoichiometry, replacing hydrogen with carbon monoxide does not seem to affect the cell widths. Thus it is possible to deduce the cell widths for 5% and 10% CO additions from the measured or calculated cell widths for a corresponding hydrogen-air or hydrogen-air-steam mixture.

## DISCUSSION

### Gaps in knowledge

Generally, data on the combustion characteristics of CO-air and CO-H<sub>2</sub>-H<sub>2</sub>O-CO<sub>2</sub>-air mixtures is scant. This is mainly because CO is not used as a commercial fuel and rarely occurs as a significant constituent in accidental gas releases in industry, and is avoided in academic studies because of its high toxicity. In the context of predicting the combustion behaviour of CO-H<sub>2</sub>-H<sub>2</sub>O-CO<sub>2</sub>-air mixtures in nuclear reactor containment buildings, there are significant gaps in the existing knowledge. Although some CO-H<sub>2</sub> combustion properties can be calculated or otherwise derived, experimental validation of the calculated values is usually needed to establish confidence in the result. At present the following information are lacking:

- Laminar and turbulent burning velocities of CO-H<sub>2</sub>-H<sub>2</sub>O-CO<sub>2</sub>-air mixtures needed as input for calculation of pressure development.
- Large-scale data on combustion pressure development in closed and vented vessels to validate predictions of combustion models applicable to CO-H<sub>2</sub>-H<sub>2</sub>O-CO<sub>2</sub>-air mixtures (small-scale data is also lacking but is not relevant for containment applications).
- Experiment data to determine the detonation cell width proportionality factor *A* for CO-H<sub>2</sub>-H<sub>2</sub>O-CO<sub>2</sub>-air mixtures.

### Safety implications of CO in containment

#### *Flammability limits*

The lean-limit concentration of hydrogen decreases as the CO concentration increases. Thus addition of 1.2% (by volume) CO to hydrogen-air mixture reduces the lean flammability for upward flame propagation from 4% to 3.61%. Addition of 6% CO requires only 2% hydrogen to become flammable. Note that the flammability of CO in air is 12.5% (by volume) for upward propagation at NTP. This means that in the presence of CO exceeding 6%, even small amounts of hydrogen (<2 vol. %) can propagate a flame. In other words, *a mixture of hydrogen and CO will have a flammability limit lower than that of either fuel*. This may be important for the combustion mitigation systems employed in the containment buildings. Similar conclusions apply to downward and horizontal limits as well as to rich limits. That is, the flammable region widens for H<sub>2</sub>-CO mixtures.

#### *Ignition temperatures*

The autoignition temperature of CO in a containment atmosphere is highly uncertain, due to the interaction of steam with the CO oxidation kinetics. Even small amounts of moisture can affect the autoignition temperature significantly. For very “dry” CO-air mixtures, the ignition temperatures are in excess of 800°C. Addition of small amounts of moisture to air drops the autoignition temperature to about

600°C. The autoignition temperature of hydrogen in air is about 580°C. Therefore, assuming water vapour is present, the autoignition temperature of hydrogen in air is practically the same as CO. Thus the presence of CO in air has no significant safety implication with respect to autoignition.

Since hot-surface ignition is related to the autoignition temperature, presence of CO in air should have no significant effect on the hot-surface ignition and effectiveness of thermal ignition devices should not be impacted.

### ***Burning velocities and combustion in vessels***

It is expected that the laminar burning velocity of hydrogen should decrease with CO addition. Because of this, the rate of pressure rise in H<sub>2</sub>-CO (and air) mixtures is expected to be slower than that in pure hydrogen (and air) but the peak pressure achievable will still be the AICC pressure for the mixture. The important point is that the *calculation of the AICC pressure must take into account the total combustible gas (H<sub>2</sub>+CO)*.

In vented vessels, the situation is complex. On one hand, the slower rate of propagation in the presence of CO could allow added time for pressure relief by venting, leading to lower peak pressures, provided the flame is laminar (and provided that CO is properly accounted in the gas composition). As always, in the presence of turbulence the outcome is not clear. Large-scale data to validate predicted pressures is not available, so significant uncertainties are carried with the calculation of combustion pressures where venting occurs to adjoining volumes.

### ***Detonability***

Addition of CO to hydrogen-air mixtures appears to increase the detonation sensitivity for a particular hydrogen concentration (naturally, the energy density of the gas is increased). At room temperature, a 10% hydrogen-air mixture will not detonate. But according to analysis 10% hydrogen-air is detonable when 5% CO is present. This may have safety implications and CO should be considered in estimating risk of detonation for local volumes.

## SUMMARY

- Flammability limits for CO-H<sub>2</sub>-H<sub>2</sub>O-CO<sub>2</sub>-air mixtures can be determined accurately from Le Chatelier's rule or from empirical curve-fits to the experimental data. The presence of CO widens the flammability limits of hydrogen.
- Burning velocities in CO, H<sub>2</sub>, steam, and air mixtures can be determined reasonably accurately at low CO concentrations using available codes. However, available codes are not reliable at low hydrogen concentrations. There is a need for experimental determination of burning velocities for CO in the range of 0 to 10% and H<sub>2</sub> in the range of 9 to 20%, and diluent (steam-CO<sub>2</sub>) concentrations of up to 50%. Because burning velocity is a basic input parameter in the calculation of combustion pressure development, and since the uncertainty in calculating burning velocity is high for the range of mixtures relevant to containment accident conditions, the gap in knowledge is significant.
- Large-scale data on combustion pressure development in closed and vented vessels is unavailable to validate predictions of combustion models applicable to CO-H<sub>2</sub>-H<sub>2</sub>O-CO<sub>2</sub>-air mixtures, resulting in significant uncertainties in predicted pressure loads from ignition.
- Experimental data on the detonation cell sizes (detonability) of CO-H<sub>2</sub> mixtures is unavailable to validate theoretical models. Since detonability is one aspect that appears sensitive to CO addition to the containment atmosphere, there are implications for reactor safety assessments.
- Theoretical studies indicate that addition of steam and CO<sub>2</sub> reduces the detonation sensitivity of CO-H<sub>2</sub> mixtures (i.e., increases the cell widths) in agreement with experimental studies in H<sub>2</sub>.
- The effect of carbon dioxide addition on cell width appears to depend on hydrogen stoichiometry—for lean hydrogen-air mixtures (the most relevant case) the cell size decreases as the CO concentration increases. For rich mixtures, the opposite is true.
- The present results indicate that the cell widths for a hydrogen-carbon monoxide-air-steam mixture can be deduced from the measured (or calculated) cell widths for a corresponding hydrogen-air-steam mixture but supporting data in CO-H<sub>2</sub> mixtures are lacking.



## REFERENCES

- Alsmeyer, H. (Chair), Proceedings of the Second CSNI Specialists Meeting on Core Debris-Concrete Interactions, Karlsruhe, Germany, 1992 April 1-3, KfK 5108, NEA/CSNI/R(92)10.
- Bull, D.C., Elsworth, J.E., Shuff, P.J. and Metcalfe, E., 1982, "Detonation Cell Structure in Fuel/Air Mixtures," *Combustion and Flame*, Vol. 45, pp. 7-22.
- Coward, H.F. and Jones, G.W., 1952, "Limits of Flammability of Gases and Vapours," Bulletin 503, U.S. Bureau of Mines.
- European Commission, Molten Corium/Concrete Interaction and Corium Coolability - a State of the Art Report, EUR 16649 EN, 1995.
- Gardiner, Jr., W.C., 1984, *Combustion Chemistry*, Springer-Verlag New York Inc., New York, New York 10010.
- Gordon, S. and McBride, B.J., 1971, "Computer Program for Calculation of Complex Chemical Equilibrium Compositions, Rocket Performance, Incident and Reflected Shocks, and Chapman-Jouguet Detonations," NASA SP-273, National Aeronautics and Space Administration, Washington, D.C.
- Guirao, C.M., Knystautas, R. and Lee, J.H., 1989, "A Summary of Hydrogen-Air Detonation Experiments," NUREG/CR—4961, SAND87—7128.
- Hustad, J.E., and Sonju, O.K., 1988, "Experimental Studies of Lower Flammability Limits of Gases and Mixtures at Elevated Temperatures," *Combustion and Flame*, Vol 71, pp. 283-294.
- Karim, G.A., Wierzba, I., and S. Boon, 1985, "Some Considerations of the Lean Flammability Limits of Mixtures Involving Hydrogen," *International Journal for Hydrogen Energy*, Vol 10, pp. 117-123.
- Kumar, R.K., 1990, "Detonation Cell Widths in Hydrogen-Oxygen-Diluent Mixtures" *Combustion and Flame*, Vol. 80, pp. 157-169.
- Kumar, R.K., 1989, "Ignition of Hydrogen-Oxygen-Diluent Mixtures Adjacent to a Hot, Nonreactive Surface," *Combustion and Flame*, Vol. 75, pp. 197-215.
- Lewis, B. and von Elbe, G., 1987, *Combustion, Flames, and Explosions of Gases*, Academic Press, Inc., Orlando, Florida 32887.
- Magzumov, A.E., Kirillov, I.A., Fridman, A.A., and Rusanov, V.D., 1995, "Influence of Carbon Monoxide Additions on the Sensitivity of the Dry Hydrogen-Air Mixtures to Detonation," *International Topical Meeting on Safety of Nuclear Power Plants*, Budapest, Hungary, September 24-27, pp. 214-216.

- Maas, U. and Warnatz, J., 1988, "Ignition Processes in carbon monoxide-hydrogen-oxygen Mixtures," In *22nd Int. Combustion Symposium*, pp. 1695-1704.
- Ritzman, R.L. (Chair), Proceedings of the CSNI Specialists Meeting on Core Debris-Concrete Interactions, Palo Alto CA, 1986 September 3-5, EPRI NP-5054-SR, 1987 February.
- Shepherd, J.E., 1985, "Chemical Kinetics and Hydrogen-Air-Diluent Detonations," In proceedings of the *10<sup>th</sup> International Colloquium on Dynamics of Explosions and Reactive Systems*, Berkeley, California, pp. 263-293.
- Snoeck, J., 1997, "Flammability Limits of a Gas Mixture," Tractebel Energy Engineering.
- Stephenson, P.L., and Taylor, R.G., 1973, "Laminar Flame Propagation in Hydrogen, Oxygen, Nitrogen Mixtures," *Combustion and Flame* 20, pp. 231-244.
- Strehlow, R.A. and Engel, C.D., 1969, "Transverse Waves in Detonations: II. Structure and Spacing in  $H_2-O_2$ ,  $C_2H_2-O_2$ ,  $C_2H_4-O_2$ , and  $CH_4-O_2$ ," *AIAA Journal*, Vol. 7, pp. 492-496.
- Tieszen, S.R., Sherman, M.P., Benedick, W.B., Knystautas, R. and Lee, J.H., 1985, "Detonation Cell size Measurements in  $H_2$ -Air- $H_2O$  Mixtures," In proceedings of the *10<sup>th</sup> International Colloquium on Dynamics of Explosions and Reactive Systems*, Berkeley, California, pp. 205-219.
- Warnatz, J., 1979, "Flame Velocity and Structure of Laminar Hydrocarbon-Air Flames," 7<sup>th</sup> ICOGER Meeting, Gottingen, Federal Republic of Germany, August 20-24.
- Westbrook, C. K. and Urtiew, P., 1982, *Nineteenth Symposium (International) on Combustion*, The Combustion Institute, Pittsburgh, Pennsylvania, pp. 615-623.
- Westbrook, C. K., 1982, "Chemical Kinetics of Hydrocarbon Oxidation in Gaseous Detonations", *Combustion and Flame*, Vol. 46, pp. 191-210.

Table 2. Reaction scheme and rate constants for carbon monoxide oxidation

REACTION	A (cm <sup>3</sup> /mol) <sup>n-1</sup> s <sup>-1</sup>	B	E/R (K)
CO + OH → CO <sub>2</sub> + H	4.4 x 10 <sup>6</sup>	1.5	-373
CO <sub>2</sub> + H → CO + OH	1.6 x 10 <sup>14</sup>	0	13230
CO + HO <sub>2</sub> → CO <sub>2</sub> + OH	1.5 x 10 <sup>14</sup>	0	11871
CO <sub>2</sub> + OH → CO + HO <sub>2</sub>	0	0	0
CO + O <sub>2</sub> → CO <sub>2</sub> + O	2.5 x 10 <sup>12</sup>	0	24055
CO <sub>2</sub> + O → CO + O <sub>2</sub>	1.69 x 10 <sup>13</sup>	0	26460
CO + O + M → CO <sub>2</sub> + M	5.3 x 10 <sup>13</sup>	0	-2285
CO <sub>2</sub> + M → CO + O	4.7 x 10 <sup>14</sup>	0	52839
CO + H + M → CHO + M	6.9 x 10 <sup>14</sup>	0	842
CHO + M → CO + H + M	7.5 x 10 <sup>14</sup>	0	8456
CO + H <sub>2</sub> → CHO + H	N/A	N/A	N/A
CHO + H → CO + H <sub>2</sub>	2 x 10 <sup>14</sup>	0	0
CO + OH → CHO + O	N/A	N/A	N/A
CHO + O → CO + OH	3 x 10 <sup>13</sup>	0	0
CO <sub>2</sub> + H → CHO + O	N/A	N/A	N/A
CHO + O → CO <sub>2</sub> + H	3 x 10 <sup>13</sup>	0	0
CO + H <sub>2</sub> O → CHO + OH	N/A	N/A	N/A
CHO + OH → CO + H <sub>2</sub> O	5 x 10 <sup>13</sup>	0	0
CO + HO <sub>2</sub> → CHO + O <sub>2</sub>	N/A	N/A	N/A
CHO + O <sub>2</sub> → CO + HO <sub>2</sub>	3 x 10 <sup>12</sup>	0	0
CH <sub>2</sub> O + H → CHO + H <sub>2</sub>	2.5 x 10 <sup>13</sup>	0	2009
CH <sub>2</sub> O + O → CHO + OH	3.5 x 10 <sup>13</sup>	0	1768
CH <sub>2</sub> O + OH → CHO + H <sub>2</sub> O	3.0 x 10 <sup>13</sup>	0	601
CH <sub>2</sub> O + HO <sub>2</sub> → CHO + H <sub>2</sub> O <sub>2</sub>	1.0 x 10 <sup>9</sup>	0	0
CH <sub>2</sub> O + M → CHO + H + M	5.0 x 10 <sup>16</sup>	0	38489
CHO + CHO → CH <sub>2</sub> O + CO	1.81 x 10 <sup>13</sup>	0	0
CHO + H → CH <sub>2</sub> O	4.68 x 10 <sup>10</sup>	0	-2285
CHO + H <sub>2</sub> → CH <sub>2</sub> O + H	1.6 x 10 <sup>11</sup>	2	8972
CHO + H <sub>2</sub> O <sub>2</sub> → CH <sub>2</sub> O + HO <sub>2</sub>	1.02 x 10 <sup>11</sup>	0	3486
CHO + H <sub>2</sub> O → CH <sub>2</sub> O + OH	5.14 x 10 <sup>11</sup>	1.35	13146

K = Reaction rate = A T<sup>B</sup> e<sup>-E/RT</sup>

M = Third body (H<sub>2</sub>, O<sub>2</sub>, CO<sub>2</sub>, CO, H<sub>2</sub>O)

N/A = Not available

N = Order of the elementary reaction; n = 2 for bimolecular and n = 3 for termolecular reactions



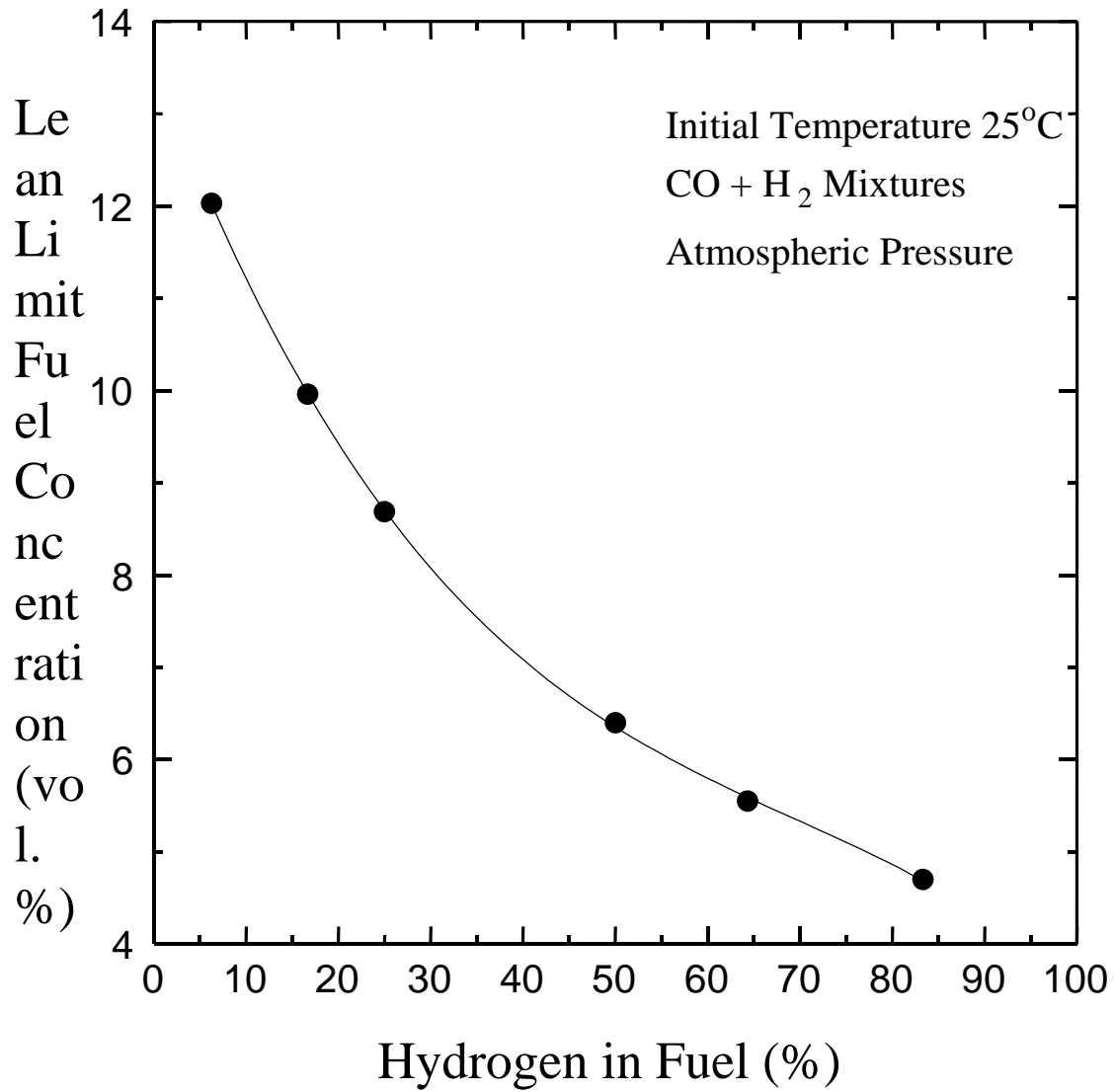


Figure 1. Variation of lean limit concentration of CO+H<sub>2</sub> mixtures with hydrogen in Fuel (data from Karim *et al.*, 1985)

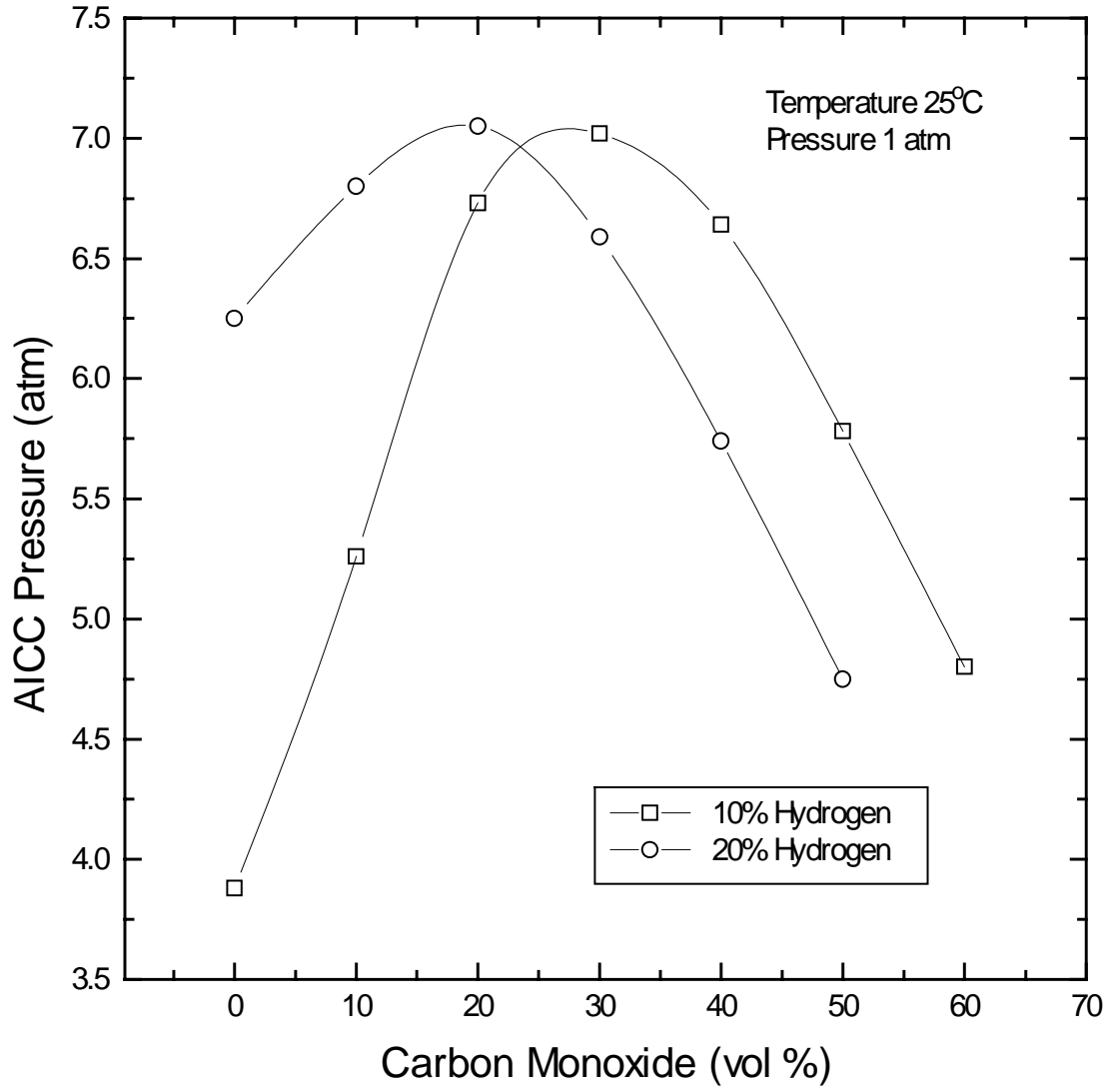


Figure 2. AICC pressures in CO-H<sub>2</sub>-air system

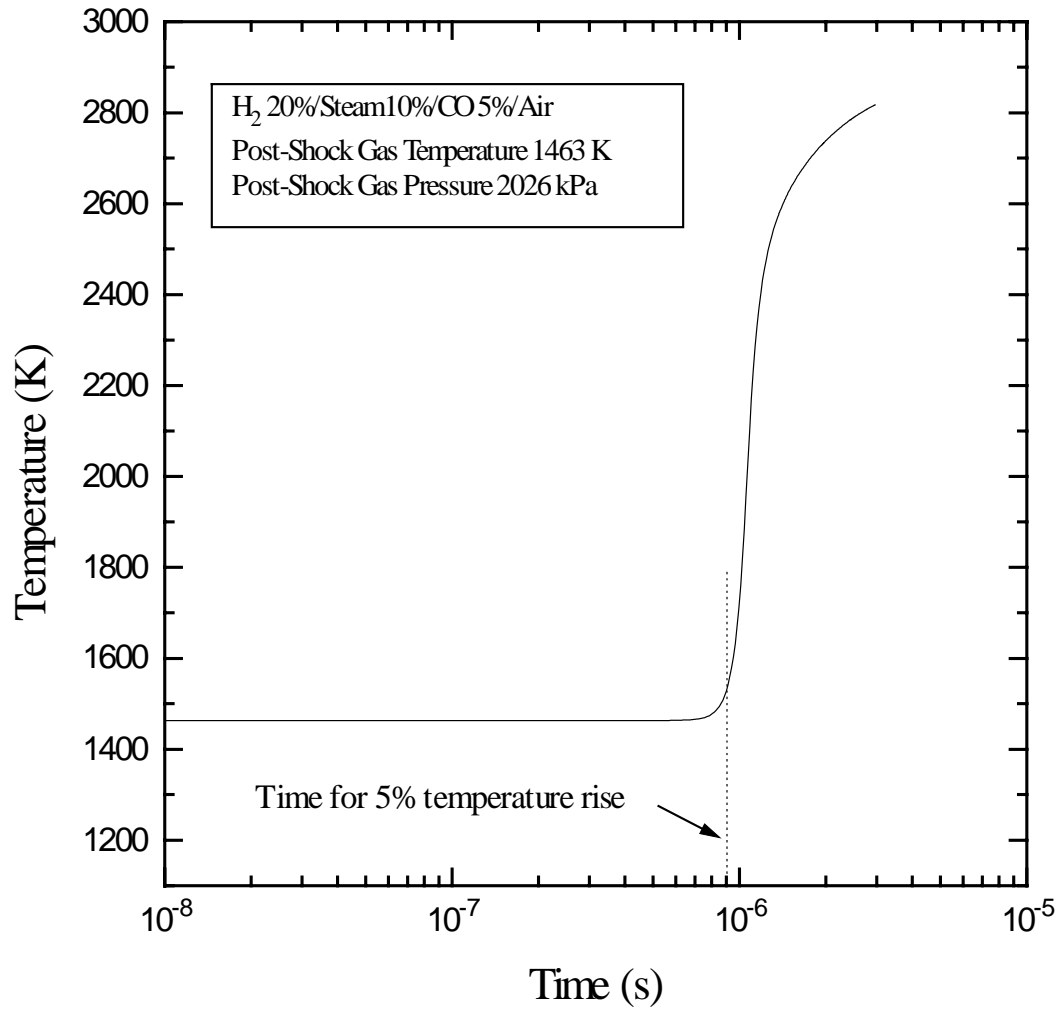


Figure 3. Typical variation of temperature with time in the shock compressed gas

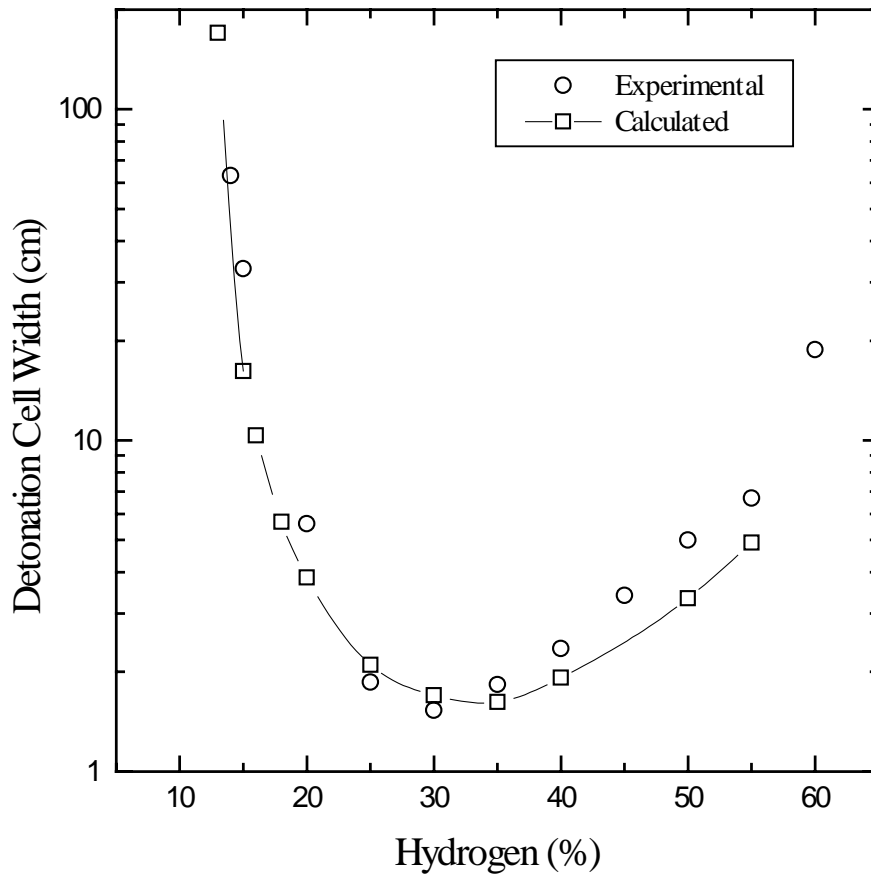


Figure 4. Comparison of measured and calculated cell widths in hydrogen-air mixtures

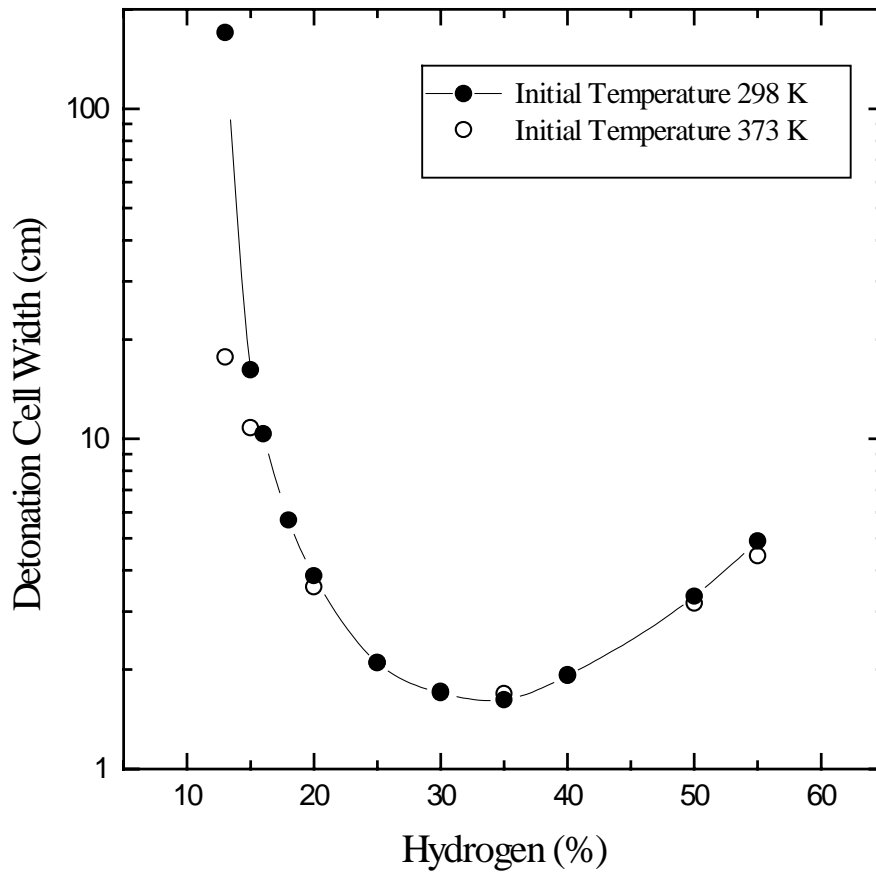


Figure 5. Effect of initial gas temperature on cell width in hydrogen-air mixtures

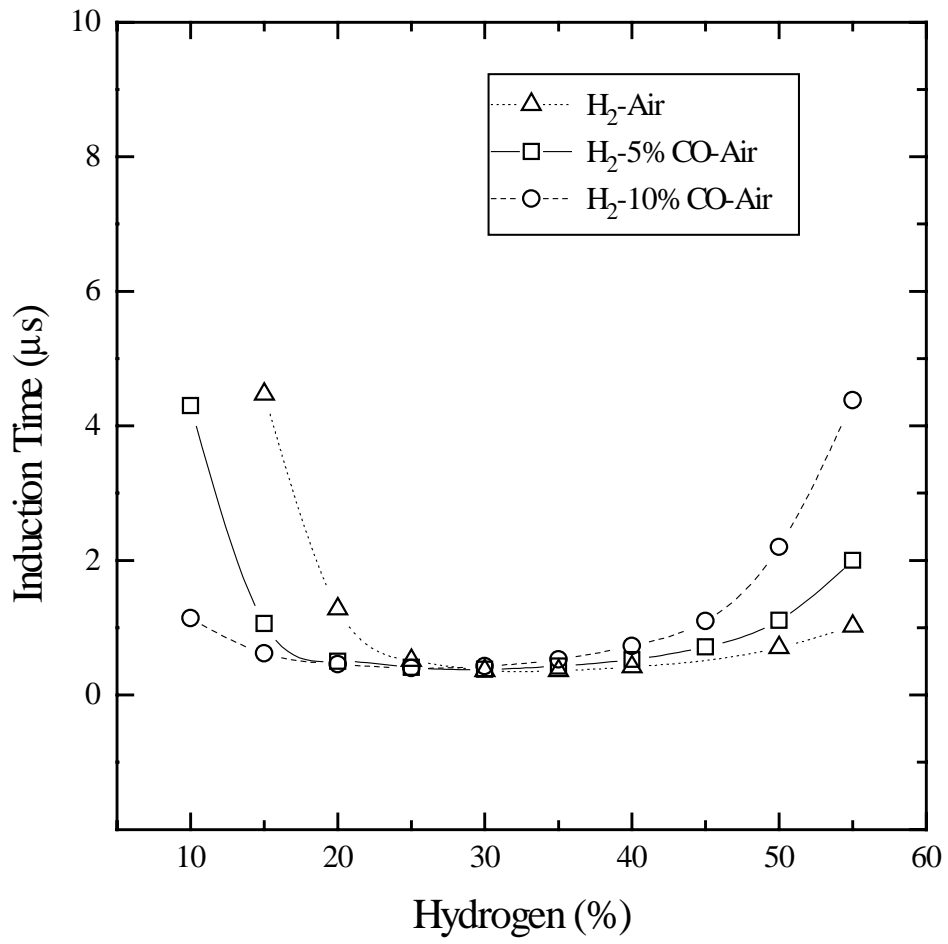


Figure 6. Effect of CO addition on induction time for hydrogen-air mixtures

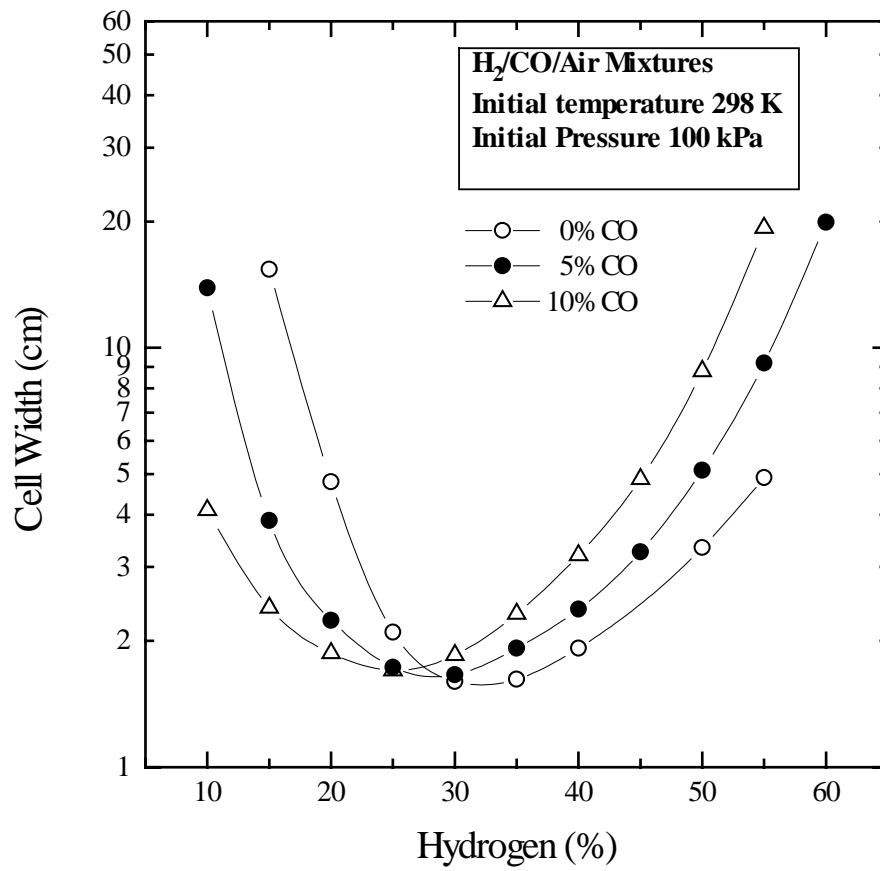


Figure 7. Effect of CO addition to hydrogen-air mixtures on cell width

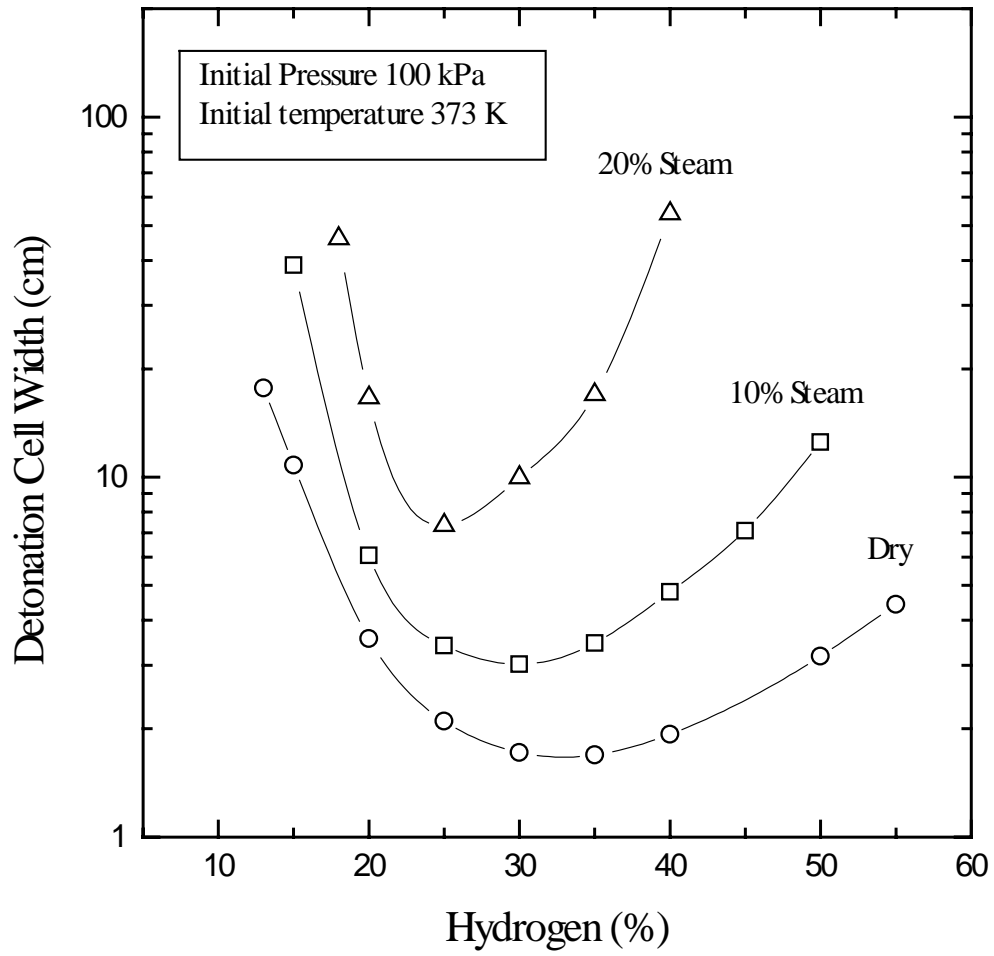


Figure 8. Effect of steam dilution on cell width for hydrogen-air mixtures

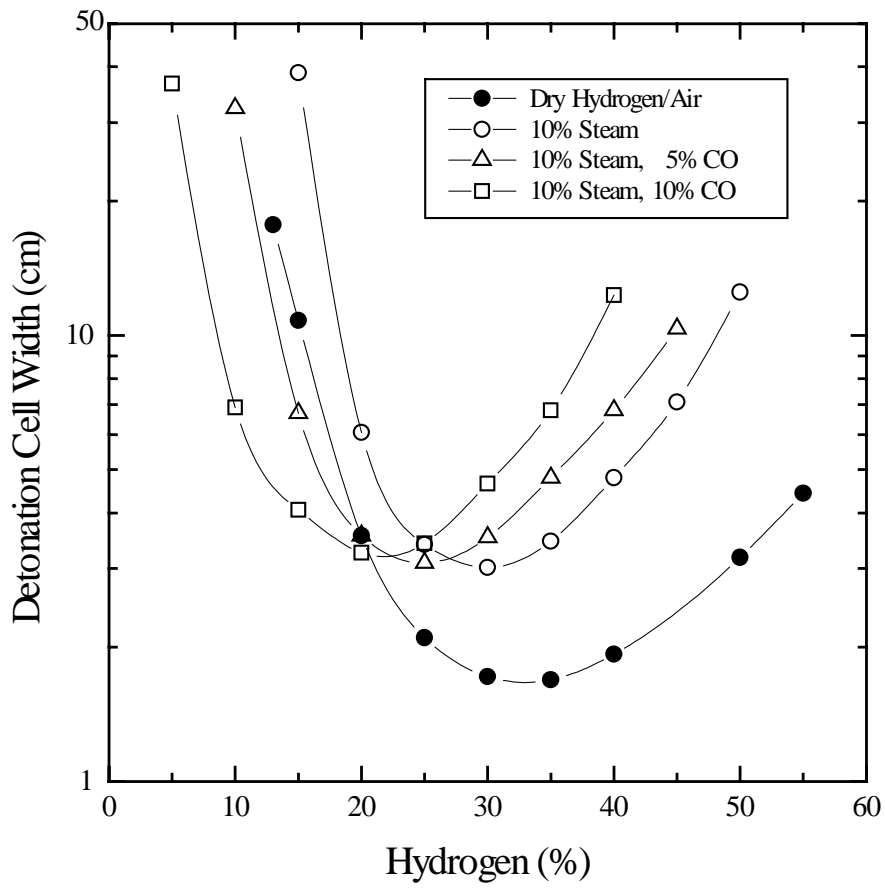


Figure 9. Effect of CO addition on cell width for hydrogen-air-10% steam mixtures.

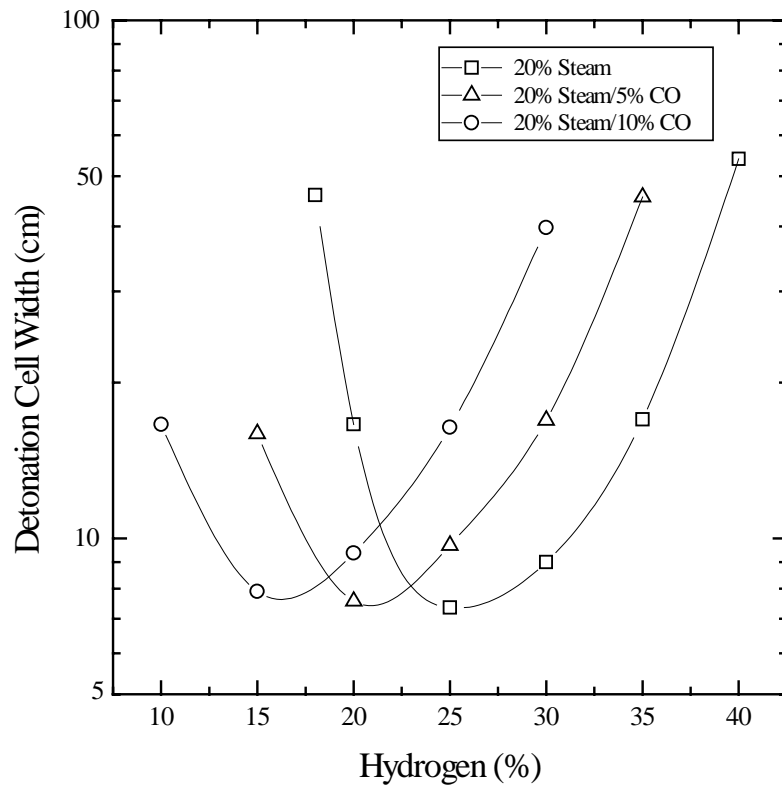


Figure 10. Effect of CO addition on cell width for hydrogen-air-20% steam mixtures

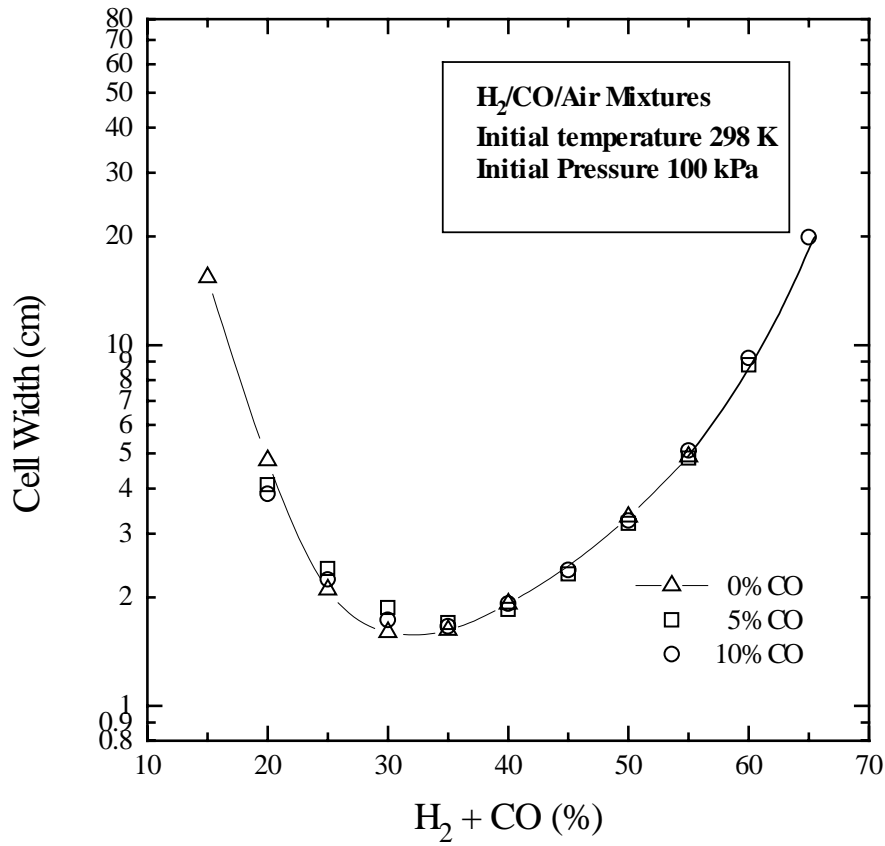


Figure 11. Cell width plotted as a function of total fuel concentration



## APPENDIX A

### CONSIDERATION OF CARBON MONOXIDE IN FRENCH SEVERE ACCIDENT STUDIES

#### A.1 Introduction

The gaseous compounds CO and CO<sub>2</sub> are formed during the interaction between corium and concrete by the decomposition of carbonates contained in this concrete and the oxidation of metals present in corium. In general, the interaction between corium and concrete takes place in two steps:

- (a) A short-term phase lasting about a quarter of an hour immediately after penetration of the vessel. During this phase, the production of inflammable gases (H<sub>2</sub> and CO) is mainly due to oxidation of zircaloy and chromium present in the corium. Since these reactions are highly exothermic, the basemat erosion speed is maximum (of the order of 1 m/h) and gases are released at high speed.
- (b) A long-term phase until the basemat is penetrated, during which inflammable gases originating from oxidation of iron originating from the initial corium and the reinforcement in the concrete. The basemat erosion speed is low (of the order of a few cm per hour) and gases are released at lower speed.

#### A.2 Composition of concrete types used in French reactor containments

Concrete used in French power stations may be siliceous or of the limestone common sand type depending on the sites and the series. Table A-1 shows the mass composition of cold concrete for the various series. Only extreme compositions are mentioned.

The concrete with the highest silicon content is in Flamanville (1,300 MWe PWR P4) and the concrete with the highest carbonate content is Gravelines units 5 and 6 (900 MWe PWR CP1-2). Two results that are important for the management of severe accidents depend on the composition of the concrete:

- (a) A siliceous concrete has a low melting enthalpy (2,180 kJ/kg) which leads to a relatively fast penetration of the basemat, but the gas production is low and does not have any significant consequences on the pressure rise in the containment.
- (b) A limestone common sand concrete has a higher melting enthalpy (2,710 kJ/kg) and a higher gas release rate than a siliceous concrete. In this case, management actions following the pressure rise in the containment take place before penetration of the basemat.

### A.3 Quantities released during corium-concrete interaction

A study was carried out in order to estimate the quantities of gas released by the corium concrete interaction. It was carried out using the WECHSL program in the ESCADRE system. This document only mentions the most important results for the 900 MWe PWR series. The following assumptions were made in this study:

- complete oxidation of the zircaloy during the accident phase in the vessel (the presence of zircaloy in the initial corium affects only the release kinetics in the short term, and does not have any effect on the total released quantity);
- the beginning of a corium concrete interaction which takes place one hour after the emergency shutdown (maximum residual power).

Two types of concrete represent extreme compositions.

The duration of the corium concrete interaction for the considered units varies between 3.5 and 4.5 days. The short-term phase lasts about fifteen minutes. During this phase, quantities of gas released into the containment depend largely on the composition of the concrete in the basemat. During this phase, the content of inflammable gases ( $H_2+CO$ ) increases globally within the containment; the molar ratio of inflammable gases to diluents ( $H_2O$  and  $CO_2$ ) varies between 5 and 2.5. This ratio reduces and the quantity of gas emitted increases as the calcium content in the concrete increases (the number of moles of combustible material is doubled and the number of moles of diluents is quadrupled).

For the long-term phase, the previous ratio becomes constant and equal to 0.2 regardless of the type of concrete being studied; the amount of diluents added is greater than the amount of combustible material added, and globally the combustible material concentration in the containment reduces. However the quantities are different; a limestone common sand concrete produces about 2.5 times more gas than a siliceous concrete while the interaction period between the corium concrete is only increased by one third.

Table A-2 gives the order of magnitude of gas flows produced in the different phases and depending on the type of concrete.

### A.4 Composition of gaseous atmosphere in the containment during corium-concrete interaction

The purpose of this section is to describe the composition of gaseous mixtures that may be encountered in the various rooms in the containment during a severe accident. An accident scenario will be chosen for this purpose, and a sensitivity study will be carried out on the concrete type considering the two extreme cases identified in the previous sections.

A type S2CD accident scenario was chosen for a 900 MWe PWR. It starts with the occurrence of a break with an equivalent diameter of 2 inches in the cold leg below the lower primary pump invert. The additional failure consists of the loss of safety injection and spray when required.

In operating procedures, the operator is required to apply primary cooling using the steam generators initially at  $56^\circ C$  per hour (5 min 38 s) and then when entering ultimate procedures (in this case U1 – 12 min 38 s) cooling becomes maximum through the atmosphere turbine by-pass system. This sequence leads to the beginning of a core meltdown at about 11 hours 45 min. Depressurization of the primary circuit through the break and the steam generators de-isolates the RIS accumulators and isolates them at a primary pressure of 15 bars after about 30 minutes. These accumulators which are not completely empty will be de-isolated on entry onto the GIAG. The core degradation finally takes place after between

12 hours and 20 hours. The vessel rupture occurs at about 20 hours. All these values were calculated with the SIPA2 simulator for the phase between the beginning of the accident and the beginning of the core meltdown and VULCAIN 7.1 in the ESCADRE system for the phase between the beginning of the core degradation and failure of the vessel.

Two corium concrete interaction calculations were then carried out using the WECHSL program in the ESCADRE system; the first using a siliceous concrete and the second using a limestone common sand concrete. This is the main parameter concerning gas quantities produced (other parameters such as the initial metal quantity or the variation in the temperature are second order parameters). Furthermore, the initial corium mass is maximum in the selected scenario, which causes the maximum release rate.

Steam has the largest quantity of energy. Other energy inputs are at about the same level, except for carbon dioxide and the radiated power for the limestone common sand case. The former is due to the large quantity of carbon dioxide produced, and the latter to the different compositions of the different types of concrete. In these calculations, the power radiated by corium and transmitted to the containment was assumed to be fixed at 15% since most of this power is actually transmitted to the walls of the reactor pit and this phenomenon was ignored in our calculations.

In the following, we consider the composition of the atmosphere in the containment for this accident scenario with these two types of concrete. The calculations were carried out using the RALOC Mod 4.0 cycle AF “lumped” parameter code with a nodalisation of the containment for a French 900 MWe PWR into 85 compartments. Only some volumes of the containment will be examined such as the R140 reactor pit, the R140B EVC duct, a reactor coolant pumps room R311 (loop No. 1 end – room located between levels 4.65 m and 16 m) and the upper compartment simulating the R800 dome.

## **Limestone common sand concrete case**

### ***Combustible concentrations***

Typical variation of CO and H<sub>2</sub> concentrations with time for a limestone common sand concrete are shown in Figure A.1. The following observations can be made:

- On average, during the high-temperature phase of the corium concrete interaction, the atmosphere in the reactor pit (R140) contains about 45% of combustible gas by volume (mostly carbon monoxide).
- Large variations are smoothed considerably in the bottom room of the reactor coolant pump (R311) and in the dome (R800). Combustible material concentrations are approximately identical for these volumes which show the beneficial mixing due to the corium-concrete interaction and the lack of a stable and long-term stratification in the containment of a French 900 MWe PWR for this type of scenario.
- The ratio between the concentrations per unit volume of hydrogen and carbon monoxide vary between 2 at the beginning of the corium-concrete interaction long-term phase (75,000 s) and almost 1 at the end of the calculation.

### ***Diluent concentrations***

Typical variation of CO<sub>2</sub> and H<sub>2</sub>O concentrations with time for a limestone common sand concrete are shown in Figure A.2. The following observations can be made:

- On average, the atmosphere in the reactor pit during the corium-concrete interaction high-temperature phase is composed of 55% of diluents. There is no air present in the reactor pit during this phase. Much larger volumes may be observed (up to 70-80% of the volume) under transient conditions.
- At the beginning of the long-term corium-concrete interaction (75,000 s), the percentage by volume of diluents drops to 44% whereas the percentage per volume of combustible gases reaches 20%. Air enters into the reactor pit during this phase.
- In the rest of the containment, volume concentrations remain uniform and the ratio between the concentrations per unit volume of steam and carbon dioxide remains constant and equal to two throughout the entire scenario starting from the beginning of the corium-concrete interaction.

### **Siliceous concrete case**

#### ***Combustible concentrations***

- In general, CO forms less than 1% by volume of the composition of the gaseous atmosphere regardless of which volume is examined. The ratio between the composition per unit volume of hydrogen and carbon monoxide reaches values exceeding 10.
- During the corium-concrete interaction short-term phase, the average composition by volume of combustible gas in the reactor pit is of the order of 47% and is composed mainly of hydrogen. The value is very similar to the case with a limestone common sand concrete. However the maximum value may be higher than in the limestone common sand case and may be almost 75% by volume of hydrogen in the reactor pit at the very beginning of the corium-concrete interaction.
- The composition by volume of combustible gas varies little during the corium concrete interaction and remains close to 20% by volume. This value is of the same order as the value obtained with the limestone common sand concrete.
- As in the case of a limestone common sand concrete, the corium-concrete interaction introduces a large amount of mixing in the containment, and no stable and long-term stratification of concentrations is observed inside the containment starting from the beginning of the corium-concrete interaction.

#### ***Diluent concentration***

- In general, the concentration of carbon dioxide per unit volume in the atmosphere in the various compartments is less than 1%, which is normal considering the quantities released for this type of concrete. For this scenario, the ratio between concentrations of steam and carbon dioxide per unit volume is always greater than 20.
- The concentration of steam in the reactor pit reaches a value of 42% by volume roughly in the middle of the corium-concrete interaction high-temperature phase. Once again, the reactor pit contains no air at the beginning of the high-temperature phase and then fills up gradually. On average, the reactor pit contains 36% of diluents, almost entirely steam, during this high-temperature phase.

In addition to the above results, Figures A.3 and A.4 show the composition of the atmosphere in terms of combustible materials ( $H_2+CO$ ) and diluents ( $H_2O+CO_2$ ) for each of the 85 compartments in the chosen model of the containment, and for 2 characteristic times in the scenario, namely the end of the corium-concrete interaction high-temperature phase (defined as being 15 minutes after the time at which the vessel ruptures) and the time corresponding to one hour of corium-concrete interaction.

A distinction can be made between several group of points shown in Figures A.3 and A.4.

First, a compartment in which the concentration of combustible materials is zero at both of these times; this compartment is disconnected from the rest of the containment for this model.

Second, the two compartments in which the concentration of diluents is always low (between 5 and 10% by volume) and the concentration of combustible materials increases slightly between these two times. These two compartments correspond to the two bottom parts of the containment for a French 900 MWe PWR which are not concerned by global convection loops inside the containment (“dead-end”). This type of geometric configuration is one of the main modelling difficulties in “points” programs such as RALOC, and their inability to calculate this type of problem correctly has often been demonstrated.

Third, there is one compartment (the reactor pit) in which the concentrations per unit volume of combustible materials and diluents is different from that in the rest of the containment. This result was described in detail in the previous sections. The difference tends to reduce as the corium concrete interaction continues.

Finally, the remaining compartments representing the containment are not affected by the transient at the beginning of the corium concrete interaction. The composition in these volumes is almost uniform represented by a dispersion around the average values equal to 5 to 10% by volume of diluents and 3 to 5% by volume of combustible material. Dispersion is greater for the first instant (end of the corium-concrete interaction high-temperature phase) than for the second instant (one hour after the beginning of the corium-concrete interaction).

## **A.5 Effects of carbon monoxide on the behaviour of catalytic recombiners**

Carbon monoxide oxidizes on platinum or palladium based catalysts in the presence of oxygen according to the following exothermic reaction:



Oxidation of carbon monoxide on the catalyst may result in partial inhibition of the catalyst with respect to oxidation of hydrogen, since CO molecules occupy some hydrogen adsorption sites.

In the H2PAR tests carried out with a SIEMENS recombiner (FR-90/150), carbon monoxide was unintentionally produced due to oxidation of the furnace graphite crucible. During these tests, an increase of about ten degrees in the temperature of catalyst plates was measured which clearly shows that CO is actually recombined into  $CO_2$  at 85°C.

Specific tests on the influence of CO were also carried out by EDF and EPRI for the purposes of the KALI experimental program. The catalytic recombiners for which the behavior was studied were of the SIEMENS or NIS type. As in a severe accident, production of CO takes place after significant production of hydrogen (preheating of the plates). During the tests, injection of CO (3% by volume) takes place after a first hydrogen injection of 4.5% by volume. The results show that the injection of CO leads to a significant increase in the hydrogen recombination rate, since CO is also consumed by the catalytic reaction. On the other hand for atmospheres with a low oxygen content (typically close to stoichiometry), the addition of

CO reduces recombination of oxygen when it drops to below 2% by volume. This effect occurs for oxygen concentrations at which the risk of explosion may be ignored.

Another point worth noting concerns poisoning of the catalyst by CO at low temperatures. At low temperatures, CO is easily adsorbed on active sites in the catalyst and inhibits the capacity of the catalyst to oxidize hydrogen. The effect disappears if the temperature increases since the CO recombines into CO<sub>2</sub>. This point is not very important for French PWRs, since CO will not be present until after a significant amount of hydrogen has been produced.

Table A-1. **Composition of concrete used in various French reactors**

Series	Site	Mass in Cold Concrete (%)				
		CaCO <sub>3</sub>	Ca(OH) <sub>2</sub>	SiO <sub>2</sub>	Free H <sub>2</sub> O	Al <sub>2</sub> O <sub>3</sub>
900 MWe PWR CP0	Siliceous	16.20	12.89	65.89	2.87	2.15
	Limestone common sand	46.86	14.02	34.20	2.59	2.32
900 MWe PWR CP1-2	Siliceous	1.07	14.72	79.38	2.42	2.41
	Limestone common sand	56.49	13.42	24.96	2.74	2.40
1,300 MWe PWR P4	Siliceous	0.87	13.69	80.53	2.67	2.23
	Limestone common sand	9.14	13.70	72.24	2.67	2.25
1,300 MWe PWR P'4	Siliceous	4.48	13.16	77.38	2.80	2.18
	Limestone common sand	30.36	13.05	51.59	2.83	2.18
1,400 MWe PWR N4	Limestone common sand	54.31	11.90	28.61	3.11	2.07

Table A-2. **Gas production rates in French reactors**

Gas	Short term		Long term	
	Limestone common sand	Siliceous	Limestone common sand	Siliceous
H <sub>2</sub>	0.6 kg/s	0.5 kg/s	0.8 g/s	2 g/s
H <sub>2</sub> O	2 kg/s	1. kg/s	60 g/s	150 g/s
CO	13 kg/s	0.2 kg/s	20 g/s	7.5 g/s
CO <sub>2</sub>	20 kg/s	0.3 kg/s	250 g/s	12 g/s

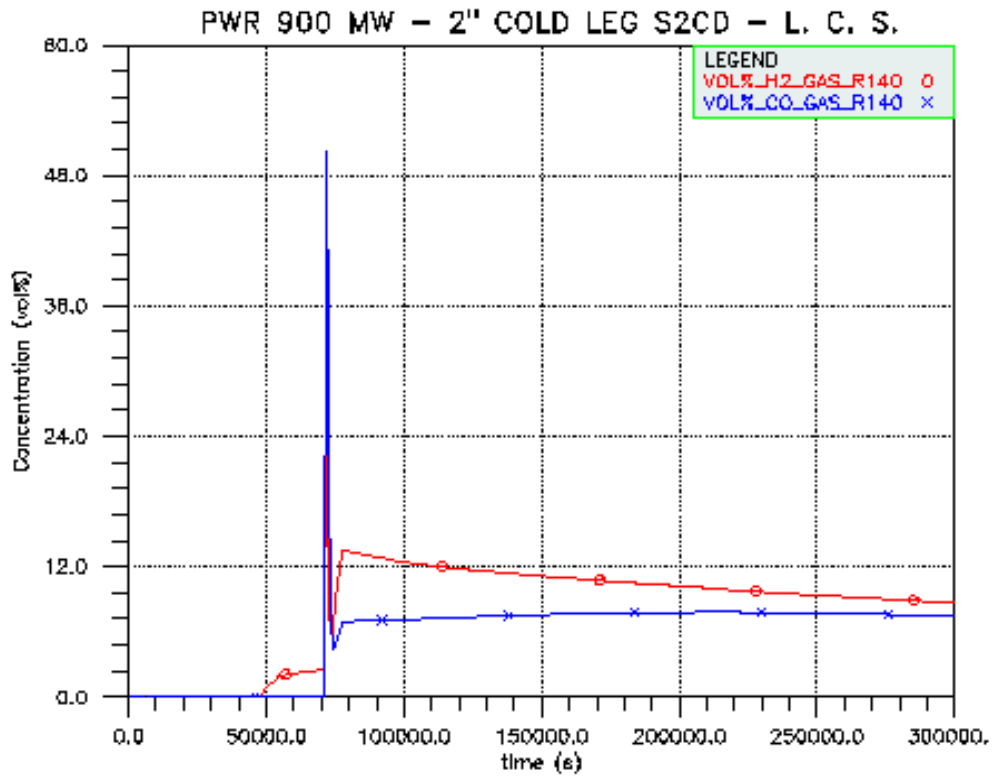


Figure A.1. H<sub>2</sub> and CO in the reactor pit - S2CD - Limestone common sand concrete

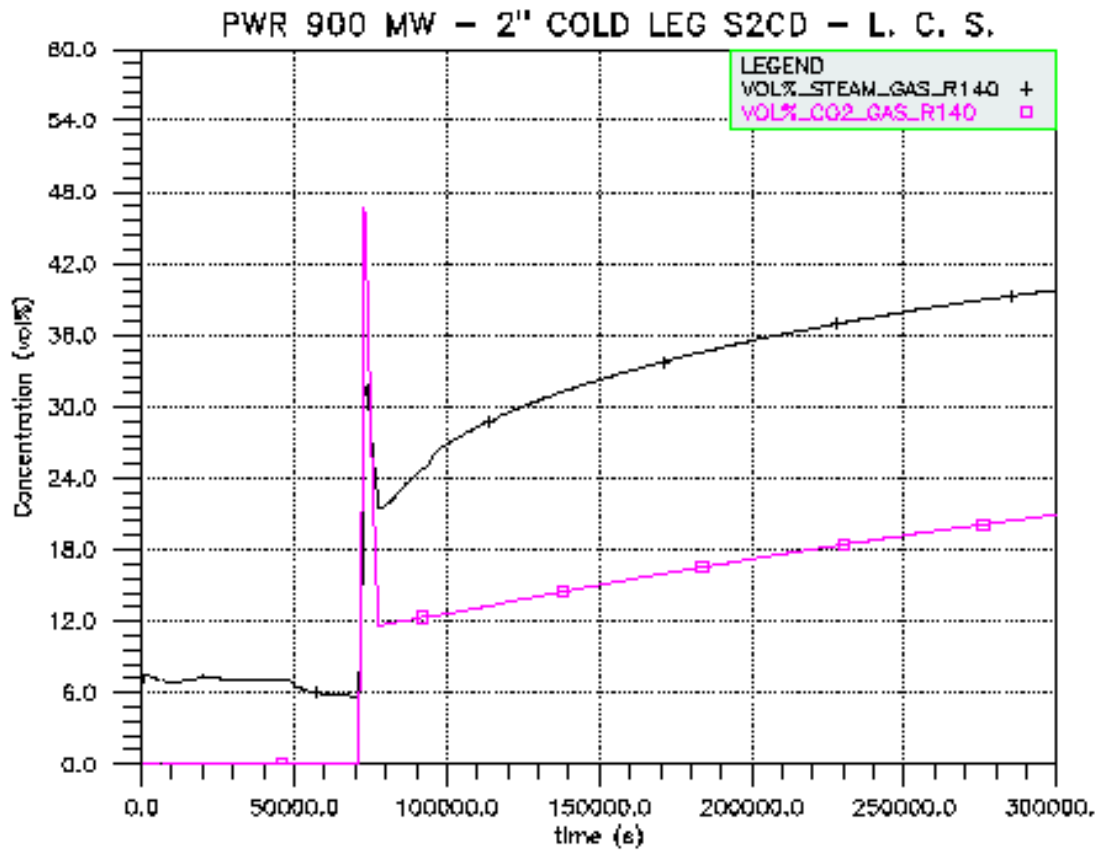


Figure A.2. H<sub>2</sub>O and CO<sub>2</sub> in the reactor pit - S2CD - Limestone common sand concrete

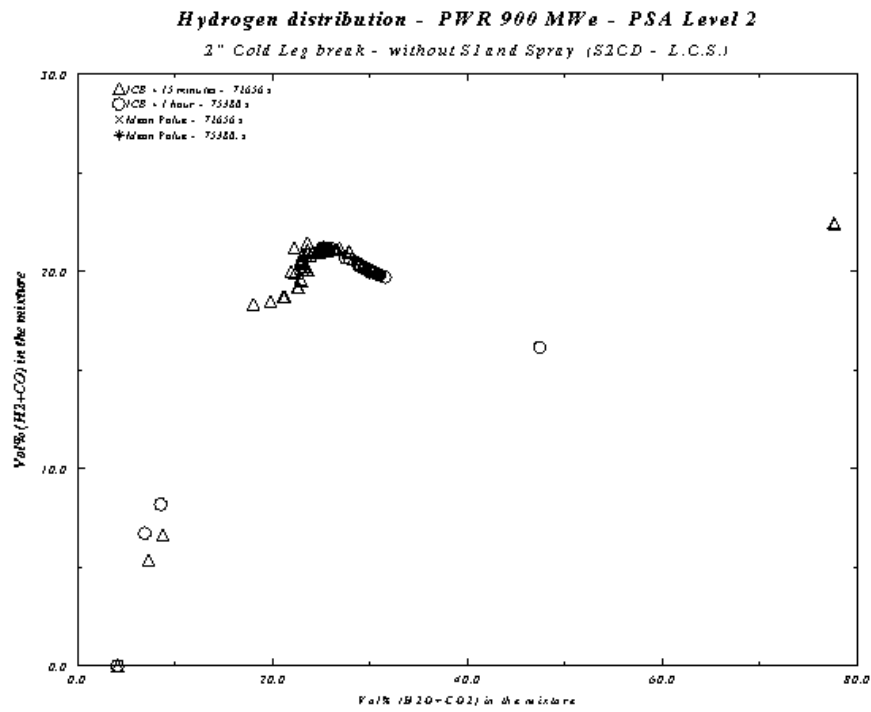


Figure A.3. H<sub>2</sub> and CO versus H<sub>2</sub>O and CO<sub>2</sub> - S2CD - Limestone common concrete

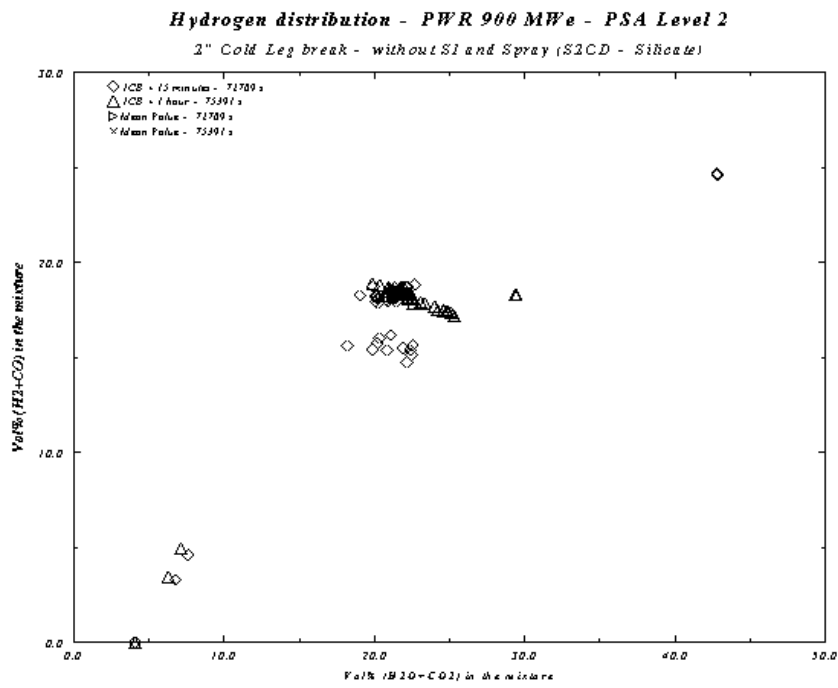


Figure A.4. H<sub>2</sub> and CO versus H<sub>2</sub>O and CO<sub>2</sub> - S2CD - Siliceous concrete